Pergamon

PII: S1040-6182(96)00060-2

Quaternary International, Vol. 40, pp. 43–52, 1997.

1040-6182/97 $32.00

LONG-PERIODIC VARIATIONS IN THE EARTH'S OBLIQUITY AND THEIR RELATION TO THIRD-ORDER EUSTATIC CYCLES AND LATE NEOGENE GLACIATIONS

L.J. Lourens and F.J. Hilgen
Department of Geology, Institute of Earth Sciences, Budapestlaan 4, 3584 CD Utrecht, The Netherlands

Evolutive spectra of four high-resolution climatic proxy records reveal that the spectral power in the obliquity frequency band increases during five well-defined intervals in the last 5.3 million years. These intervals correspond to periods of high-amplitude variations in the tilt (obliquity) of the Earth's axis, connected with a 1.2 myr cycle, and to sea-level lowstands of third-order eustatic cycles in the Haq *et al.* (1987) curve. This implies that the development of major Plio–Pleistocene glaciations proceeded episodically and that third-order cycles are glacio-eustatically controlled. In (at least) two of these intervals sinistrally-coiled neogloboquadrinids entered the Mediterranean at times of glacial periods. One interval starts around 2.8 Ma and is characterized by the first occurrence of *N. atlantica* (s). Another interval begins at the Plio–Pleistocene boundary around 1.8 Ma and is characterized by the common occurrence of sinistrally-coiled *N. pachyderma*. Also during the late Miocene third-order cycles correlate well with the 1.2 myr cycle of obliquity. A significant drop in the third-order eustatic curve starting at the Tortonian–Messinian boundary, for instance, coincides with a period of high-amplitude variations in the obliquity time series connected with the 1.2 myr cycle. © 1997 INQUA/ Elsevier Science Ltd. All rights reserved.

INTRODUCTION

What caused the onset of major northern hemisphere glaciations around 2.8 million years ago? This question has gained considerable scientific interest during the last decade, because the history of the onset is now being documented in unprecedented detail in continuous deep marine sequences. But despite the high-resolution records and the application of increasingly sophisticated climate models, this question has not yet been answered satisfactorily. Some researchers focus on the continuously changing positions of the Earth's continents and oceans and argue that the opening and closing of isthmuses could create critical 'gateways' for altering oceanic circulation and hence climate. The final closure of the Panama Isthmus occurred shortly before the glacial era began (Keigwin, 1978; Marshall, 1988; Keller *et al.*, 1989) and may have led to an increase of North Atlantic Deep Water production, due to enhanced flux of relatively warm and high saline surface waters to the high latitude eastern Atlantic. The oceanic heat loss from NADW formation was released to the atmosphere over the Norwegian–Greenland Sea resulting in mild winter temperatures and large volumes of precipitation required for the development of continental ice caps. Recent investigations of benthic foraminiferal $\delta^{13}C$ from several ODP sites, however, provide no evidence for a progressively increasing ventilation of NADW as would be expected, but rather point to a decrease in NADW and/or NAIW production during this transition (Tiedemann, 1991; Raymo *et al.*, 1992).

Alternatively, the onset of major northern hemisphere glaciations has been explained by a long-term decline in the concentration of atmospheric carbon dioxide. This would reduce the amount of heat trapped in the atmosphere and, as a consequence, lead to 'greenhouse' cooling (Chamberlin, 1899; Vincent and Berger, 1985). Following this line of reasoning, an increase in productivity between 3.2 and 2.4 Ma resulted in a decrease of atmospheric CO_2, thus, creating a planetary balance in favour of glaciations (Sarnthein and Fenner, 1988). On even longer time scales CO_2 is removed from the atmosphere by burial of organic carbon and by weathering of silicate rocks to form carbonates. Acceleration in seafloor spreading rates and associated mountain uplift may have caused the increase in chemical weathering of silicate-bearing (volcanic and basement) rocks needed to reduce the atmospheric CO_2 concentration and, hence, global cooling (Raymo *et al.*, 1988). In addition, uplift of the Himalayan–Tibetan plateau and southwestern North America may have created favourable atmospheric conditions for the development of ice caps over eastern Canada, Scandinavia and Siberia (Ruddiman and Kutzbach, 1989). On the other hand, subduction releases CO_2 into the atmosphere through volcanic activity. A deceleration in seafloor spreading would, therefore, reduce the volcanic CO_2 release and lead to favourable conditions for glaciations as well. Application of the astronomical calibrated polarity time scale (APTS) (Shackleton *et al.*, 1990, 1995a; Hilgen, 1991a, b), however, revealed no significant changes in seafloor spreading rates in four out of five plate pairs during the critical interval between 4 and 2 million years ago (Wilson, 1993). Moreover, it has been questioned (Molnar and England, 1990) whether the apparent accelerations in late Cenozoic uplifts are real or whether the geological and palynological evidence is merely a product of the climate change itself. Raymo (1991) cites the sharp rise in $^{87}Sr/^{86}Sr$ during the Neogene as evidence for uplift. She also notes, however, that global episodes of glaciations coincide with most of the rises in $^{87}Sr/^{86}Sr$ during the Phanerozoic (see also Miller *et al.*, 1991).

In the present paper we will show that the onset of major northern hemisphere glaciations is at least partially controlled by long-periodic variations in the Earth's obliquity. Moreover, the long-term obliquity variations seem to determine the temporal occurrence of glacial episodes and associated third-order eustatic cycles.

CLIMATIC EVOLUTION DURING THE PLIO–PLEISTOCENE

Recently four high-resolution and astronomically-dated climatic proxy records have been established for the (major part of the) last 5.3 million years. These records are the benthic $\delta^{18}O$ record of ODP site 659 from the equatorial Atlantic (Tiedemann *et al.*, 1994) and of ODP sites 677 and 846 from the equatorial Pacific (Shackleton and Hall, 1989; Shackleton *et al.*, 1990, 1995a, b), and the planktonic $\delta^{18}O$ and Sea Surface Temperature (SST) records from the Mediterranean (Lourens *et al.*, 1996a) (Fig. 1). Evolutive spectral analyses are applied to depict the temperal evolution of the SST and $\delta^{18}O$ records and, hence, to determine shifts in the relative contribution of spectral peaks in the different orbital frequency bands (Fig. 2).

Precession

Figure 2 clearly illustrates that the planktonic $\delta^{18}O$ record from the Mediterranean is strongly influenced by precession throughout the studied interval, whereas the influence of this cycle on the benthic $\delta^{18}O$ records from the equatorial Atlantic and Pacific is only recorded in the last million years. In the open ocean the precession component reflects above all global variations in ice volume and occurs superimposed on the prominent 100 kyr glacial cycles (Imbrie *et al.*, 1984) (see also Fig. g2",0>). In the Mediterranean, the precession component in $\delta^{18}O$ is closely related to lithology (Lourens *et al.*, 1992, 1996a, b): $\delta^{18}O$ minima coincide with sapropels in the upper Pliocene and/or grey-coloured beds of the lower Pliocene carbonate cycles. The $\delta^{18}O$ minima most probably reflect an increase in wetness of circum-Mediterrancan climate and continental runoff (Rossignol-Strick, 1983; Gudjonsson and van der Zwaan, 1985; Lourens *et al.*, 1992). Evidently, precession-related variations in the Mediterranean record precede, those in the open ocean, indicating that both global and Mediterranean climatic systems operate at least partly independently.

Obliquity

The influence of obliquity is intermittently recorded in all climatic proxies throughout the studied interval. In contrast with the precession-induced variations, the influence of obliquity is recorded almost synchronously in all records, indicating that we are dealing with a climatic signal of global importance. Obliquity-related variations in the benthic $\delta^{18}O$ records from the open ocean have been interpreted to reflect primarily changes in global ice volume (e.g. Shackleton *et al.*, 1990, 1995b; Raymo *et al.*, 1989; Tiedemann *et al.*, 1994). Obliquity-related variations in the Mediterranean $\delta^{18}O$ record have been interpreted in a similar way, but in this case the signal is amplified due to regional changes in sea surface salinity and/or temperature (Hilgen *et al.*, 1993). Obliquity-related variations in SST occur in phase with ^{18}O, indicating that the glacial cycles affected SST conditions in the Mediterranean as well (Lourens *et al.*, 1992).

Around 2.8 million years ago, a relative increase in power of the spectral peak in the obliquity frequency band can be observed. This increase is attributed to the onset of major northern hemisphere glaciations. Between 2.8 Ma and the present, three intervals can be distinguished in the evolutive spectra in which the power of the obliquity peak is enhanced. These intervals are seperated by two intervals in which the power is strongly reduced. Close inspection of the obliquity time series (Fig. 2) reveals that the time series is similarly marked by three intervals with relatively high-amplitudinal variations separated by two intervals with low-amplitudinal variations. These long-periodic variations in obliquity are linked to a 1.2 myr cycle, which modulates the higher frequency variations in the obliquity time series (Fig. 3). Between 5.3 and 2.8 Ma, two additional intervals with relatively high amplitude variations can be distinguished in the obliquity time series (Fig. 2). Again, there is some evidence that during these intervals the power in the obliquity frequency band of the $\delta^{18}O$ and SST spectra increases, although these increases are far less pronounced than in the younger interval. The increases can best be observed in the evolutive spectra of the benthic $\delta^{18}O$ records from the Atlantic and Pacific, although the power remains low between 4.5 and 2.8 Ma. During this time interval, however, the high-amplitude variations in obliquity related to the 1.2 myr cycle are suppressed due to the occurrence of a modulation term with an even longer period (Fig. 3).

The observed long-periodic amplitudinal variations in the power of the spectral peaks in the obliquity frequency band may, however, be explained as an artifact which results from the astronomical tuning of the climatic proxy records to (among others) obliquity itself. In general, the coherence with the target curve will increase with the number of age controlpoints derived from astronomical tuning (Shackleton *et al.*, 1995c) and, as a result, the evolutive spectrum of climatic proxy records will start to mimic that of the target (in this case the 65°N summer insolation curve). For this purpose we recalculated the evolutionary spectrum of the benthic $\delta^{18}O$ records from the equatorial Pacific (Fig. 2: Pacific*), but this time we applied only six calibration points to construct the $\delta^{18}O$ time series. The resulting evolutive spectrum resembles the one based on the orbitally-tuned time series,

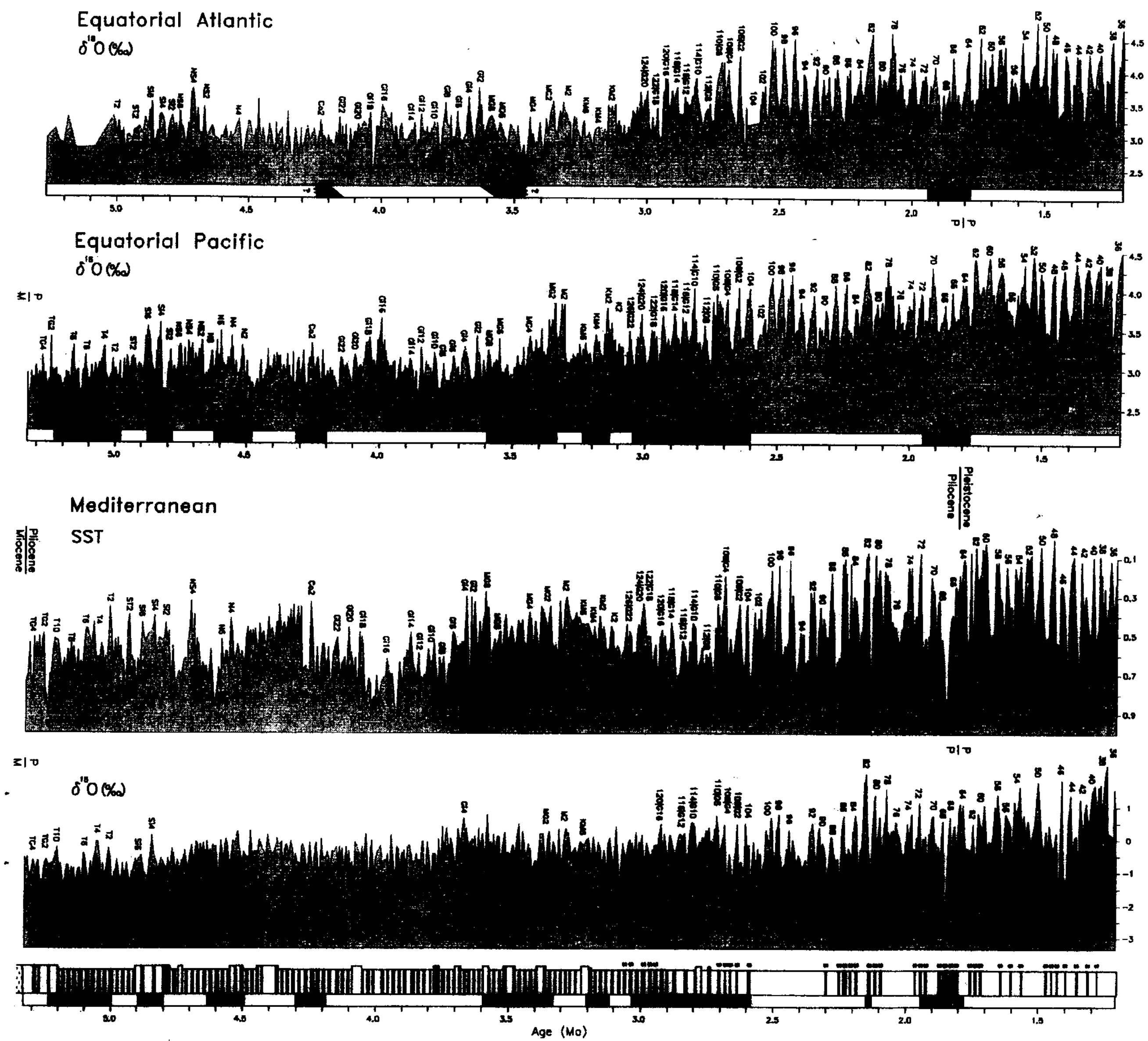

FIG. 1. Comparison between the SST and $\delta^{18}O$ record of the Mediterranean (Lourens *et al.*, 1996a) and the $\delta^{18}O$ records of ODP sites 677 and 846 (Shackleton and Hall, 1989; Shackleton *et al.*, 1995b) and 659 (Tiedemann *et al.*, 1994). The SST record is based on the ratio warm versus cool- and warm-water species as dicussed in the text. The oxygen isotopic stage codification is after Ruddiman *et al.* (1989), Raymo *et al.* (1989), Tiedemann *et al.* (1994) and Shackleton *et al.* (1995b).

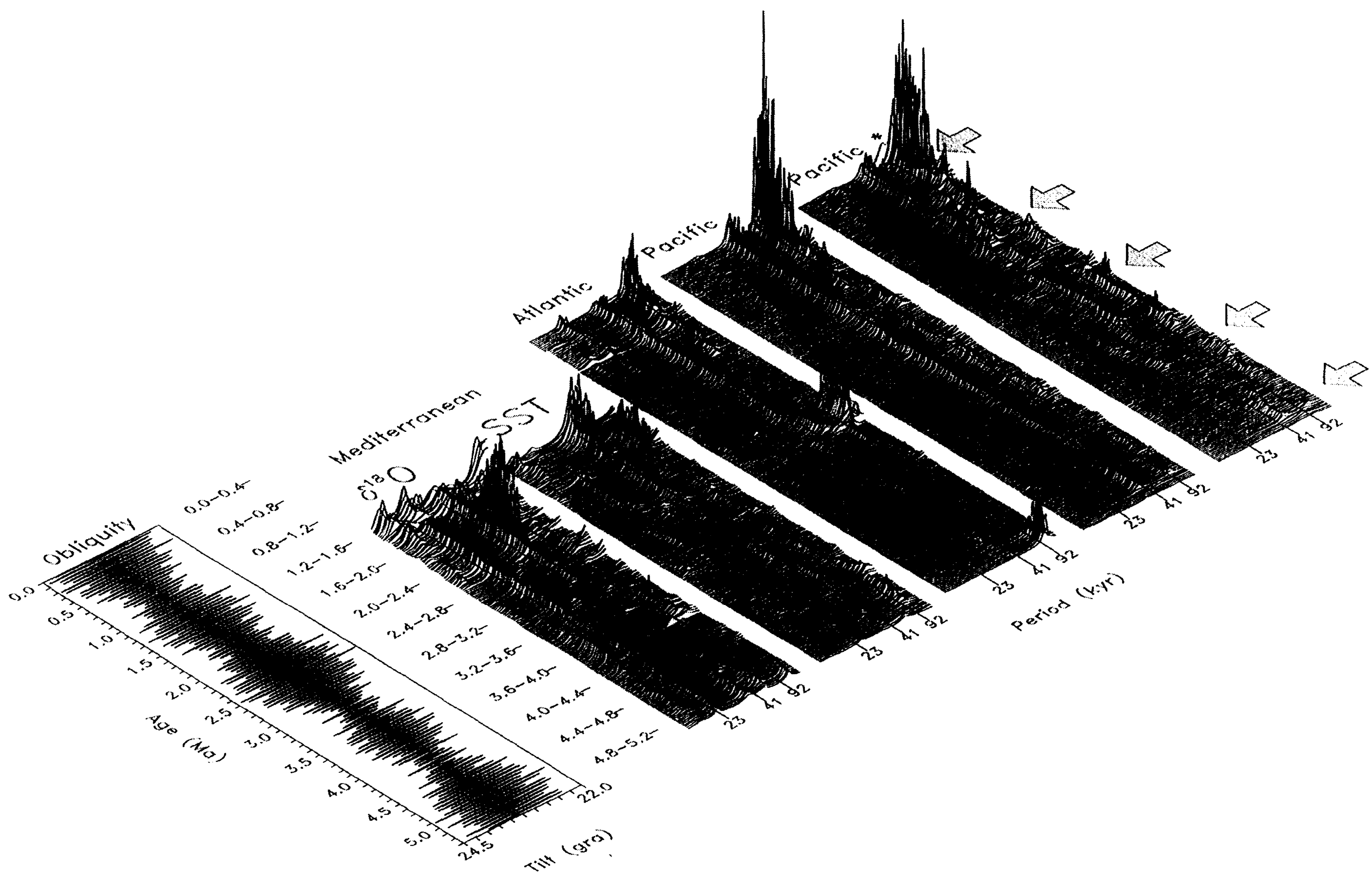

FIG. 2. Comparison between the evolutive spectra of the benthic $\delta^{18}O$ record of the equatorial Atlantic ODP site 659 (Tiedemann *et al.*, 1994), the composite benthic $\delta^{18}O$ record of the equatorial Pacific ODP sites 677 and 846 (Shackleton and Hall, 1989; Shackleton *et al.*, 1990, 1995b) and the planktonic $\delta^{18}O$ and Sea Surface Temperature records of the Mediterranean (Lourens *et al.*, 1996a), and the obliquity time series (Laskar, 1988; Laskar *et al.*, 1993) for the last 5.3 million years. The power spectrum estimation is based on the maximum entropy (all poles) method (Numerical Recipes, Chapter 12.8) with *M* (= constant) is 80, the step between successive spectra is 20 kyr, and the window of a spectrum is 400 kyr. Arrows indicate periods marked by relatively large amplitude fluctuations in obliquity caused by a 1.2 myr modulation. To make sure that the observed long-period variations in the power of the spectral peaks in the obliquity frequency band are not simply an artifact resulting from the astronomical tuning of the climatic proxy records to (among others) obliquity itself we constructed an alternative time series of the equatorial Pacific $\delta^{18}O$ record (Pacific*). Time controlpoints of Pacific* in site 677 are: 0 (mbst)=0 (ka), 30.31=780.93, 72.40=1777.81, and time controlpoints in site 846 are: 63.43 (mbst)=1763 (ka), 100.75=2600, 143.45=3594 and 203.31=5239.

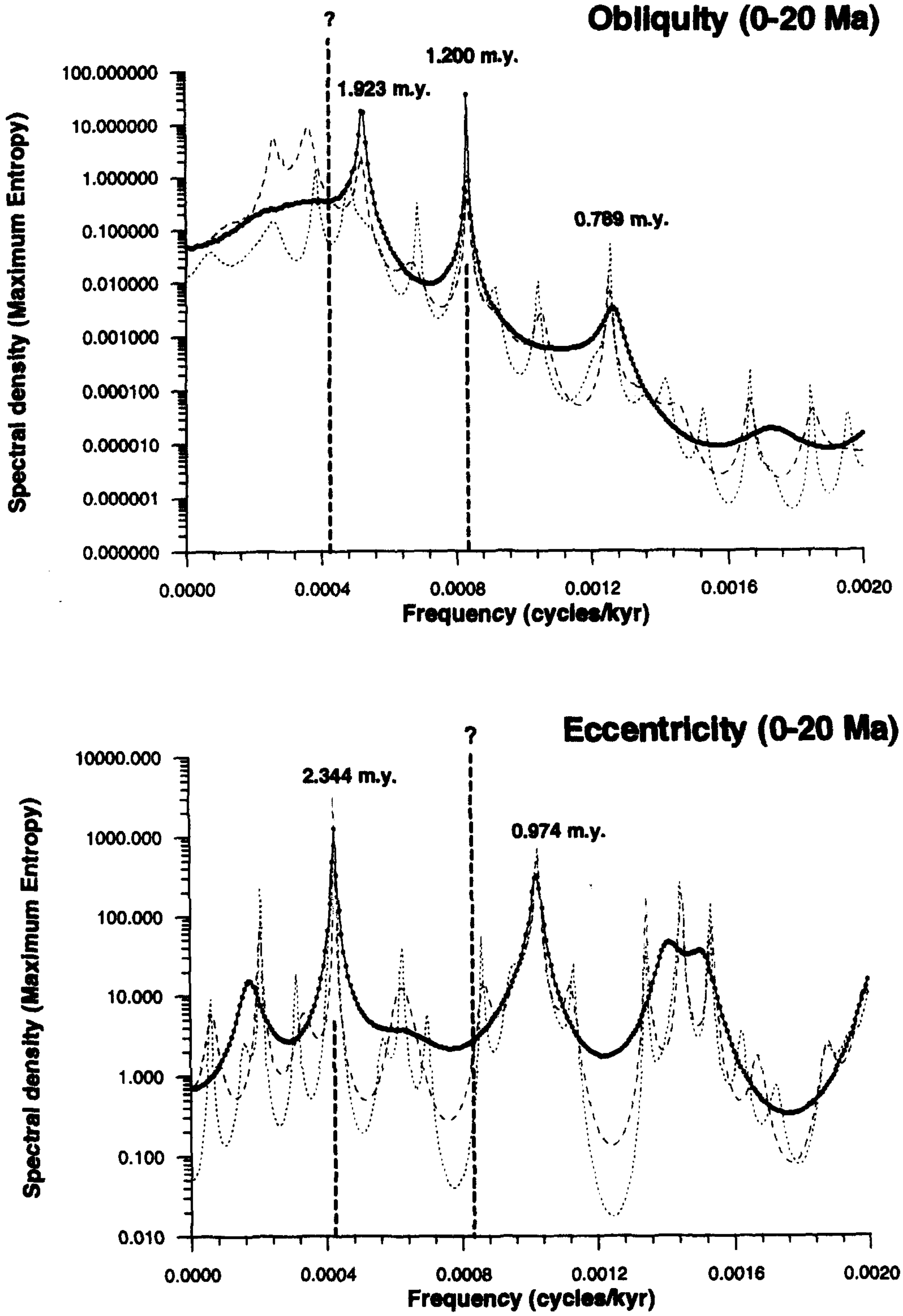

FIG. 3. Spectral estimates of the La90 (Laskar *et al.*, 1993) obliquity and eccentricty time series (normalized) of the last 20 million years. The power spectrum estimation is based on the maximum entropy (all poles) method (Numerical Recipes, Chapter 12.8) with N=20,001 (amount of data points) M=4000 (solid), 8000 (dashed) and 12,000 (dots).

indicating that the long-periodic variations in the obliquity frequency band are most likely not caused by the tuning procedure.

THIRD-ORDER EUSTATIC CYCLES

Several mechanisms such as glacial eustasy (Vail *et al.*, 1977; Haq *et al.*, 1987) for specific geological time periods, stress release at plate margins (Cloetingh, 1992), tectononism (Galloway, 1989a, b), geoidal eustasy (Mörner, 1987; Sabadini *et al.*, 1990), or even impacts of hypervelocity asteroids and/or comets (Kendall *et al.*, 1995) have been proposed to explain third-order sequences, which last on the average 1–3 million years. We compared the third-order sequences of Haq *et al.* (1987) with the long-periodic variations in the Earth's obliquity in Fig. 4. In this figure, we refrained from using the standard obliquity time series, but preferred to use the time series of successive obliquity minima for the Earth's

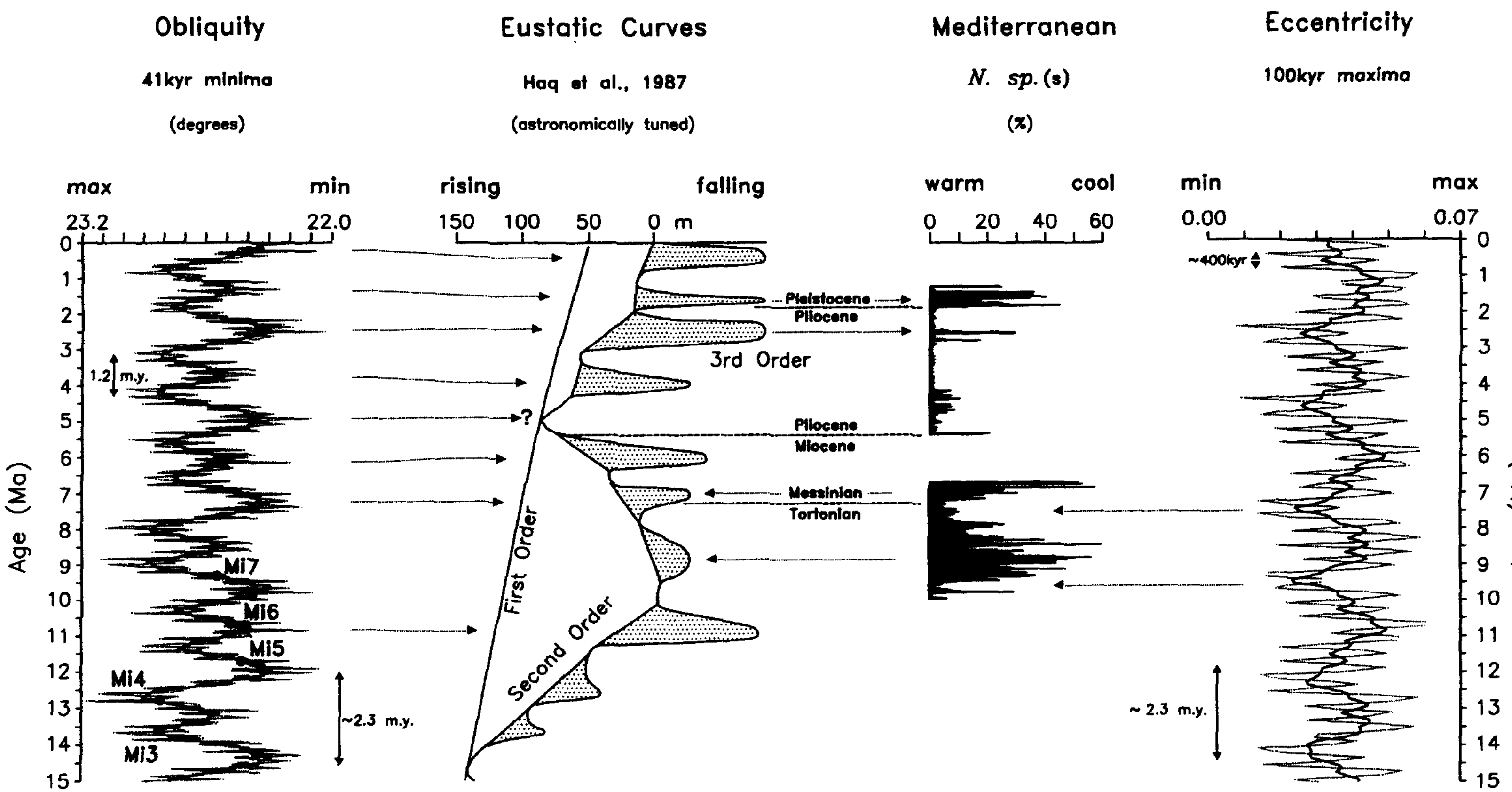

FIG. 4. Comparison between (a 5 point moving average of and) obliquity and eccentricity minima, the — eustatic — sea level curve of Haq *et al.* (1987) for the last 15 million years, and abundance pattern of sinistrally-coiled neogloboquadrinids in the Mediterranean (Lourens *et al.*, 1996a, b). Mi3–Mi7 indicate glacial periods in the Miocene after Miller *et al.* (1991) with ages based on the polarity time scale of Cande and Kent (1992). The 3rd-order eustatic curve of Haq *et al.* (1987) has been recalibrated to the astronomical time scale (Shackleton *et al.*, 1990; Hilgen, 1991a, b; Hilgen *et al.*, 1995; Lourens *et al.*, 1996a) for the last 9.7 million years and to the polarity time scale (Cande and Kent, 1992) for the time interval between 9.7 and 15 Ma.

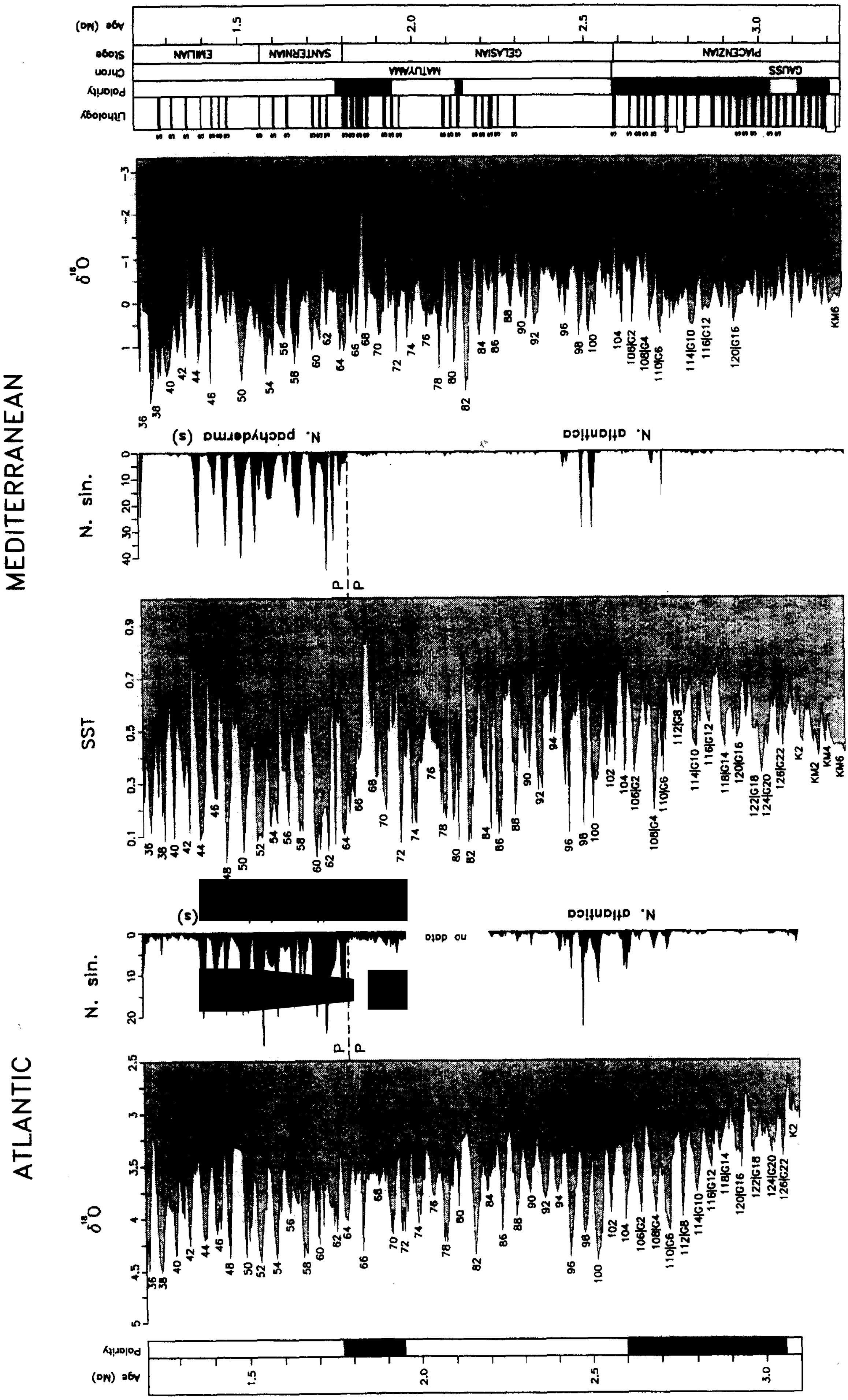

FIG. 5. Comparison between the SST, $\delta^{18}O$ and sinistrally-coiled neogloboquadrinid records of the Mediterranean (Lourens *et al.*, 1996a) and the $\delta^{18}O$ (Raymo *et al.*, 1989) and sinistrally-coiled neogloboquadrinid records of DSDP site 607. The sinistrally-coiled neogloboquadrinid records comprises the sum of *N. pachyderma* (s) and *N. atlantica* (s) and is based on data of Ruddiman *et al.* (1986), Lourens *et al.* (1996a)Lourens *et al.* (1996b) and Lingen and Lourens (work in progress). P/P marks the Plio–Pleistocene boundary as defined at the top of sapropel e in the Vrica section (Aguirre and Pasini, 1985).

axis. This time series may give an even better notion of glacial episodes and, hence, sealevel lowstands, because individual glacial cycles correspond to obliquity minima (Hays *et al.*, 1976).

Plio–Pleistocene

The comparison reveals that at least for the last 5 million years long-periodic variations in obliquity (minima) correlate well with the third-order eustatic cycles, indicating that these (third-order) cycles correspond to glacial episodes and, hence, that they may be glacio-eustatically-controlled. Significant drops in the sea level curve of Haq *et al.* (1987) around 2.8, 1.7 and 0.7 Ma coincide with important shifts toward more arid climatic conditions in Africa and major steps in the evolution of African hominids and other vertebrates (deMenocal, 1995). In the Mediterranean, the significant global climatic cooling around 2.8 million years ago is marked by the first occurrence of *N. atlantica* during Oxygen Isotopic Stage 110 (Lourens *et al.*, 1996a). This species, indigenous to the North Atlantic mid- to high-latitude, repeatedly invaded the Mediterranean during glacials connected with high-amplitude obliquity variations in the latest Gauss to earliest Matuyama until its extinction at the end of Isotopic Stage 96 (Zachariasse *et al.*, 1990) (Fig. 5).

The Plio–Pleistocene boundary — as defined at the top of sapropel *e* in the Vrica section (Sicily, Italy) (Aguirre and Pasini, 1985) — is also marked by an increase in the abundance of a left-coiling neogloboquadrinid species, *N. pachyderma* (s) (Fig. 5). This increase starts during Oxygen Isotope Stage 64 and occurred synchronously in the Mediterranean and adjacent Atlantic Ocean. Similarly *N. atlantica, N. pachyderma* (s) abundances increased during obliquity-controlled glacials (Lourens *et al.*, 1996b). The inferred climatic cooling associated with the Plio–Pleistocene boundary in the Mediterranean (Colalongo *et al.*, 1982; Combourieu-Nebout *et al.*, 1990) coincides with the beginning of the last but one third-order eustatic sea level fall around 1.7 Ma (Fig. 4), indicating that the boundary marks a major step in global cooling connected with the 1.2 myr cycle as well.

The last third-order eustatic sea level fall around 0.7 Ma coincides with the (mid-Pleistocene) transition of dominantly obliquity-controlled glacial cycles to the 100 kyr glacial cycles of the late Pleistocene (e.g. Ruddiman *et al.*, 1989). The cause of the 100 kyr cycles is still a matter of debate. A direct response to eccentricity forcing seems unlikely also because at that time the magnitude of the 100 kyr eccentricity cycle starts to decline (see Fig. 3 and Imbrie *et al.* (1993) for a review). Alternatively, internal nonlinear processes within the climate system have been proposed to be responsible for the observed 100 ka glacial cycles (cf. Imbrie and Imbrie, 1980; Oerlemans, 1980; Pollard, 1983; Salzman, 1987). On the other hand Ruddiman *et al.* (1989) hinted that the prominent shift towards the 100 kyr cyclicity is triggered by some additional change, probably tectonics. It is, however, remarkable that during this interval the amplitudinal variations in obliquity connected with the 1.2 myr cycle starts to increase (Fig. 4). The increase in the amplitude of the obliquity cycle may have favoured (1) a long-term increase of the ice-sheets needed to explain the increase in the 100 kyr^{-1} frequency band by nonlinear climate response (cf. Imbrie *et al.*, 1993), or (2) a change in the frequency of the obliquity cycle which may have triggered a strong 100-kyr forcing of the climate (Liu, 1992).

Miocene

Third-order eustatic cycles correlate well with the 1.2 myr cycle in the Earth's obliquity during the late Miocene, whereas this correlation becomes less obvious for the time interval prior to 8.5 Ma (Fig. 4). There is, however, evidence that the 1.2 myr cycle of obliquity also played a role during this time interval. In the first place, the average duration of the Mi-3 to Mi-7 glacial ($\delta^{18}O$) events (Miller *et al.*, 1991; Oslick *et al.*, 1994) dated at 13.6, 12.8, 11.7, 10.5 and 9.3 Ma (ages after Cande and Kent, 1992) is close to 1.2 Ma. Secondly, Beaufort (1994) showed that amplitude variations of a 100 kyr cyclicity in two detailed and continuous 16 myr long Miocene climatic proxy records (reflecting migrations of the Antarctic polar front and associated variations in paleoproductivity near Kerguelen Island) fluctuate quasi-periodically with periods of 2.38, 1.14 and 0.8 Ma, close to the long-term periods of eccentricity and obliquity. In addition, the amplitude variations of the 100 kyr cycles are enhanced during the Mi1–Mi6 cooling periods, indicating that the 100 kyr cycle was strengthened at times of glacial expansion just as they were during the late Pleistocene. Beaufort noted that the long-periodic variations in obliquity and eccentricity are identical, suggesting that the quasi-periodic fluctuations in the amplitude of the 100 kyr cyclicity are controlled by either obliquity or eccentricity or by a combination of both.

The similarity of the long-periodic variations may result from a strict resonance in the leading terms of eccentricity and inclination systems ($2E_3$–$2E_4$=I_3–I_4) and seems to be a common feature of the inner planets of the solar system (Laskar, 1988). Spectral analysis of the obliquity and eccentricity time series, however, reveals that the periods and power of the long-term variations in the spectra of both records are not the same (Fig. 3). For instance, the obliquity spectrum reveals strong peaks centered at 1.2 and 0.8 million year periods, whereas the eccentricity spectrum shows two strong peaks at 2.344 and 0.974 million years. But the influence of a ~2.3 myr cycle is well reflected in the obliquity time series as an alternation of high- and low-amplitude minima (Fig. 4). We plotted the time series of successive eccentricity minima in Fig. 4 to illustrate the difference in the long-periodic variations of the Earth's eccentricity and obliquity. This figure clearly shows that long-periodic variations in eccentricity are dominated by a ~2.3 million year cycle and not by a 1.2 million year cycle.

In Fig. 4 we also show the abundance pattern of left-coiling neogloboquadrinids in the Mediterranean late Miocene (after Antonarakou *et al.*, work in progress). High percentages of left-coiling neogloboquadrinids in the late Miocene may indicate relatively cool periods and associated sealevel lowstands if the long-term variations in this record are interpreted in a similar way as for the Plio–Pleistocene. Surprisingly, these long-term variations correlate well with the third-order eustatic cycles, suggesting that also the late Miocene third-order cycles correspond to cool (glacial) episodes and, as a consequence, are glacio-eustatically-controlled. For instance, the Tortonian–Messinian boundary coincides with the base of a significant sealevel fall and is marked by a strong increase of left-coiling neogloboquadrinids in the Mediterranean. Again, this level corresponds with the beginning of an interval with high-amplitude variations in obliquity connected with the 1.2 myr cycle. Comparison with the long-term orbital variations further reveals that the ~2.3 myr cycle has largely contributed to the long-term variations in left-coiling neogloboquadrinids and third-order cycles in this time interval (Fig. 4), suggesting that these fluctuations are controlled by either obliquity or eccentricity or by a combination of both.

The influence of the ~2.3 myr cycle in eccentricity is at least observed in the (dominantly precession-controlled) sapropel patterns of the Mediterranean during the late Neogene. Deviating sapropel clusters occur around 2.6, 7.4 and 9.5 Ma (Hilgen, 1991a; Hilgen *et al.*, 1995) that lack the usually pronounced expression of the 100 kyr cycle due to the occurrence of the ~2.3 myr cycle. Hilgen (1991a) used this relationship as a first-order correlation to construct the astronomical time scale for the late Pliocene to early Pleistocene.

In addition, the duration of many (third-order) sequences and geological stages in the Paleozoic and Mesozoic is often within the 1–4 Ma range of long-period orbital variations (e.g. Ramsbottom, 1977; De Boer, 1983; Ferry and Rubino, 1987; see also Schwarzacher, 1993). It has been hypothesized that these stages and sequences are (indeed) connected with long-term orbital variations, especially with a ~2.0 myr eccentricity cycle. However, the 1.2 myr cycle is held responsible for the (glacial eustatic) third-order sequences of the Plio–Pleistocene.

ACKNOWLEDGEMENTS

We thank J.P. Van Dijk for interesting discussions. P.G. Sjoerdsma is thanked for his assistance in preparing the computer program. We are grateful to A. Antonarakou and W.J. Zachariasse for providing their preliminary results of the Miocene planktonic foraminiferal data. This study was partly funded by The Netherlands Organization for Scientific Research (NWO grant to L.J. Lourens).

REFERENCES

Aguirre, E. and Pasini, G. (1985). The Pliocene–Pleistocene boundary. *Episodes*, **8**, 116–120.

Beaufort, L. (1994). Climate importance of the modulation of the 100 kyr cycle inferred from 16 m.y. long Miocene records. *Paleoceanography*, **9**, 821–834.

Cande, S.C. and Kent, D.V. (1992). A new geomagnetic polarity time scale for the Late Cretaceous and Cenozoic. *Journal of Geophysical Research*, **97**, 13917–13951.

Chamberlin, T.C. (1899). An attempt to frame a working hypothesis of the cause of glacial periods on an atmospheric basis. *Journal of Geology*, **7**, 545–584, 667–685, 751–787.

Cloetingh, S.P. (1992). Lithospheric dynamics and the tectonics of sedimentary basins. *Proceedings of Koninklijke Nederlandse Akademie van Wetenschappen Amsterdam*, **95**, 349–369.

Colalongo, M.L., Pasini, G., Pelosio, G., Raffi, S., Rio, D., Ruggieri, G., Sartoni, S., Selli, Selli and Sprovieri, R. (1982). The Neogene/Quaternary Boundary definition: a review and proposal. *Geographie Fisica Dinamique Quaternary*, **5**, 59–68.

Combourieu-Nebout, N., Semah, F. and Djubiantonola, T. (1990). Limite Pliocène-Pléistocène: précisions magnétostratigraphiqucs et climatiques par l'étude sériée de la coup-type de Vrica (Crotone, Italie). *Comptes Rendus de l'Academie des Sciences, Series II*, **311**, 851–857.

De Boer, P.L. (1983). Aspects of middle Cretaceous pelagic sedimentation in southern Europe. *Geologica Ultraiectina*, **31**, 112.

deMenocal, P.B. (1995). Plio–Pleistocene African climate. *Science*, **270**, 53–59.

Ferry, S. and Rubino, J.L. (1987). La modulation eustatique du signal orbital dans les sédiment pélagiques. *Comptes Rendus de l'Academie des Sciences*, **305**, 477–482.

Galloway, W. (1989). Genetic stratigraphic sequences in basin analysis *I: Architecture and genesis of flooding-surface bounded depositional units. The American Association of Petroleum Geologists Bulletin*, **73**, 125–142.

Galloway, W. (1989). Genetic stratigraphic sequences in basin analysis *II: Application to Northwest Gulf of Mexico Cenozoic Basin. The American Association of Petroleum Geologists Bulletin*, **73**, 143–154.

Gudjonsson, L. and van der Zwaan, G.J. (1985). Anoxic events in the Pliocene Mediterranean: stable isotope evidence of run-off. *Proceedings of the Koninklyke Nederlandse Akademie van Wetenschappen*, **88**, 69–82.

Haq, B.U., Hardebol, J. and Vail, P.R. (1987). Chronology of fluctuating sea levels since the Triassic. *Science*, **235**, 1156–1167.

Hays, J.D., Imbrie, J. and Shackleton, N.J. (1976). Variations in the Eanh's orbit: Pacemaker of the ice ages. *Science*, **194**, 1121–1132.

Hilgen, F.J. (1991). Astronomical calibration of Gauss to Matuyama sapropels in the Mediterranean and implication for the geomagnetic polarity time scale. *Earth and Planetary Science Letters*, **104**, 226–244.

Hilgen, F.J. (1991). Extension of the astronomically calibrated (polarity) time scale to the Miocene/Pliocene boundary. *Earth and Planetary Science Letters*, **107**, 349–368.

Hilgen, F.J., Lournes, L.J., Berger, A. and Loutre, M.F. (1993). Evaluation of the astronomically calibrated time scale for the late Pliocene and earliest Pleistocene. *Paleoceanography*, **8**, 549–565.

Hilgen, F.J., Krijgsman, W., Langereis, C.G., Lourens, L.J., Santarelli, A. and Zachariasse, W.J. (1995). Extending the astronomical (polarity) time scale into the Miocene. *Earth and Planetary Science Letters*, **136**, 495–510.

Imbrie, J. and Imbrie, J.Z. (1980). Modeling the climate response to orbital variations. *Science*, **207**, 943–953.

Imbrie, J., Hays, J.D., Martinson, D.G., McIntyre, A., Mix, A.C., Morley, J.J., Pisias, N.G., Prell, W.L. and Shackleton, N.J. (1984). The orbital theory of Pleistocene climate: Support from a revised chronology of the marine $\delta^{18}O$ record. *In*: Berger, A. *et al.* (eds), *Milankovitch and Climate*, pp. 269–305. D. Reidel, Norwell.

Imbrie, J., Berger, A., Boyle, E.A., Clemens, S.C., Dully, A., Howerd, W.R., Kukla, G., Kutzbach, J., Martinson, D.G., McIntyre, A., Mix, A.C., Molfino, B., Morley, J.J., Peterson, L.C., Pisias, N.G., Prell, W.L., Raymo, M.E., Shackleton, N.J. and Toggweiler, J.R. (1993). On the structure and origin of major glaciation cycles: the 100,000-year cycle. *Paleoceanography*, **8**, 699–736.

Keller, G., Zenker, C.E. and Stone, S.M. (1989). Late Neogene history of the Pacific-Caribbean gateway. *Journal of South American Earth Sciences*, **2**, 73–108.

Keigwin, L.D. (1978). Pliocene closing of the Isthmus of Panama. based on biostartigraphic evidence from nearby Pacific cores and Caribbean Sea cores. *Geology*, **6**, 630–634.

Kendall, C.G.St.C., Levine, P.A. and Ehrlich, R. (1995). The enigma of third-order sea level cycles: A cosmic connection? *In*: Haq, B.Q. (ed.), *Sequence Stratigraphy and Depositional Response to Eustatic, Tectonic and Climatic Forcing*, pp. 367–376. Kluwer Academic.

Laskar, J. (1988). Secular evolution of the solar system over 10 million years. *Astronomy and Astrophysics,* **198,** 341–362.

Laskar, J., Joutel, F. and Boudin, F. (1993). Orbital, precessional, and insolation quantities for the Earth from -20 Myr to +10 Myr. *Astronomy and Astrophysics,* **270,** 522–533.

Liu, H.-S. (1992). Frequency variations of the Earth's obliquity, and the 100-kyr ice-age cycles. *Nature,* **358,** 397–399.

Lourens, L.J., Hilgen, F.J., Gudjonsson, L. and Zachaflasse, W.J. (1992). Late Pliocene to early Pleistocene astronomically forced sea surface productivity and temperature variations in the Mediterranean. *Marine Micropaleontology,* **19,** 49–78.

Lourens, L.J., Hilgen, F.J., Antonarakou, A., Van Hoof, A.A.M., Vergnaud-Grazzini, C. and Zachariasse, W.J. (1996a). Evaluation of the Pliocene to early Pleistocene astronomical time scale. *Paleoceanography,* **11,** 391–413.

Lourens, L.J., Hilgen, F.J., Raffi, I. and Vergnaud-Grazzini, C. (1996b). Early Pleistocene chronology of the Vrica section (Calabria, Italy). *Paleoceanography,* **11,** 797–812.

Marshall, L.G. (1988). Land mammals and the great American interchange. *American Science,* **76,** 380–388.

Miller, K.G., Clement, B.M., Feigenson, M.D. and Wright, J.D. (1991). Miocene isotope reference section, Deep Sea Drilling Project Site 608: An Evaluation of isotope and biostratigraphic resolution. *Paleoceanography,* **6,** 33–52.

Molnar, P. and England, P. (1990). Late Cenozoic uplift of mountain ranges and global climate change: chicken or egg?. *Nature,* **346,** 29–34.

Mörner, N.A. (1987). Pre-Quaternary long-term changes in sea level. *In*: Devoy, R.J.N. (eds), *Sea Surface Studies, A Global View*, pp. 242–263. Croom Helm, New York.

Oerlemans, J. (1980). Model experiments on the 100,000-yr glacial cycle. *Nature,* **287,** 430–432.

Oslick, J.S., Miller, K.G., Feigenson, M.S. and Wright, J.D. (1994). Oligocene–Miocene strontium isotopes: correlations to an inferred glacio-eustatic record. *Paleoceanography,* **9,** 427–443.

Pollard, D. (1983). Ice-age simulations with a calving ice-sheet model. *Quaternary Research,* **20,** 30–48.

Ramsbottom, W.H.C. (1977). Major cycles of transgression and regression (mesothems) in the Namurian. *Proceedings of the Geological Society of Yorkshire,* **41,** 261–291.

Raymo, M.E. (1991). Geochemical evidence supporting T.C. Chamberlin's theory of glaciation. *Geology,* **19,** 344–347.

Raymo, M.E., Ruddiman, W.F. and Froelich, P.N. (1988). Influence of late Cenozoic mountain building on ocean geochemical cycles. *Geology,* **16,** 649–653.

Raymo, M.E., Ruddiman, W.F., Backman, J., Clement, B.M. and Martinson, D.G. (1989). Late Pliocene variation in northern hemisphere ice sheets and north Atlantic deep water circulation. *Paleoceanography,* **4,** 413–446.

Raymo, M.E., Hodell, D. and Jansen, E. (1992). Response of deep ocean circulation to initiation of northern hemisphere glaciation (3–2 Ma). *Paleoceanography,* **7,** 645–672.

Rossignol-Strick, M. (1983). African monsoons, an immediate climatic response to orbital insolation. *Nature,* **303,** 46–49.

Ruddiman, W.F. and Kutzbach, J.E. (1989). Forcing of late Cenozoic northern hemisphere climate by plateau uplift in southern Asia and the American West. *Journal of Geophysical Research,* **94,** 18409–18427.

Ruddiman, W.F., McIntyre, A. and Raymo, M. (1986). Paleoenvironmental results from North Atlantic sites 607 and 609. *Initial Report Deep Sea Drilling Project,* **94,** 855–878.

Ruddiman, W.F., Raymo, M.E., Martinson, D.G., Clement, B.M. and Backman, J. (1989). Pleistocene evolution: Northern hemisphere ice sheets and the North Atlantic Ocean. *Paleoceanography,* **4,** 353–412.

Sabadini, R., Doglioni, C. and Yuen, D.A. (1990). Eustatic sea level fluctuations induced by polar wander. *Nature,* **345,** 708–710.

Salzman, B. (1987). Carbon dioxide and the $\delta^{18}O$ record of late Quaternary climatic change: A global model. *Climate Dynamics,* **1,** 77–85.

Sarnthein, M. and Fenner, J. (1988). Global wind induced change of deep-sea sediment budgets, new ocean production and CO_2 reservoirs ca. 3.3–2.35 Ma BP. *Philosophical Transactions of the Royal Society of London,* **B318,** 487–504.

Schwarzacher, W. (1993). Cyclostratigraphy and the Milankovitch theory. *Developments in Sedimentology,* **52,** 240.

Shackleton, N.J. and Hall, M.A. (1989). Stable isotope history of the Pleistocene at ODP site 677. *In*: Becker, K. and Sakai, H. *et al.* (eds), *Proc. ODP, Sci. Results, 111*, pp. 285–316. College Station, TX (Ocean Drilling Program).

Shackleton, N.J., Berger, A. and Peltier, W.R. (1990). An alternative astronomical calibration of the lower Pleistocene time scale based on ODP Site 677. *Transactions of the Royal Society of Edinburgh,* **81,** 251–261.

Shackleton, N.J., Crowhurst, S., Hagelberg, T., Pisias, N.G. and Schneider, D.A. (1995a). A new late Neogene time scale: Application to leg 138 sites. *In*: Pisias, N.G., Mayer, L.A. and Janecek, T.R. *et al.* (eds), *Proc. ODP, Sci. Results, 138*, pp. 73–101. College Station, TX (Ocean Drilling Program).

Shackleton, N.J., Hall, M.A. and Pate, D. (1995b). Pliocene stable isotope stratigraphy of ODP site 846. *In*: Pisias, N.G., Mayer, L.A. and Janecek, T.R. *et al.* (eds), *Proc. ODP, Sci. Results, 138*, pp. 337–353. College Station, TX (Ocean Drilling Program).

Shackleton, N.J., Hagelberg, T.K. and Crowhurst, S.J. (1995). Evaluating the success of astronomical tuning: Pitfalls of using coherence as a criterion for assessing pre-Pleistocene timescales. *Paleoceanography,* **10,** 693–697.

Tiedemann, R. (1991). Acht millionen yahre klimageschichte yon Nordwest Afrika und Paläo-Ozeanographie des angrenzenden Atlantiks: Hochauflösende Zeitreihen von ODP-Sites 658-661. *Berichte-Reports, Geologish Paläontologishes Institut der Universität Kiel,* **46,** 190.

Tiedemann, R., Sarnthein, M. and Shackleton, N.J. (1994). Astronomical time scale for the Pliocene Atlantic $\delta^{18}O$ and dust flux records of ODP site 659. *Paleoceanography,* **9,** 619–638.

Vail, P.R., Mitchum, R.M., Jr, Todd, R.G., Widmier, J.M., Thompson, S. III, Sangree, J.B., Bubb, J.N. and Hatlelid, W.G. (1977). Seismic stratigraphy and global changes of sea level. *In*: Payton, C.E. (ed.), *Seismic Stratigraphy — Applications to Hydrocarbon Exploration, American Association of Petroleum Geologists Memoir 26*, 49–212.

Vincent, E. and Berger, W.H. (1985). Carbon dioxide and polar cooling in the Miocene: The Montery Hypothesis. *In*: Sundquist, E.T. and Broecker, W.S. (eds), *The Carbon Cycle and Atmospheric CO_2: Natural Variations Archean to Present*, pp. 455–468. American Geophysical Union, Washington, DC.

Wilson, D.S. (1993). Confirmation of the astronomical calibration of the magnetic polarity timescale from sea-floor spreading rates. *Nature,* **364,** 788–790.

Zachariasse, W.J., Gudjonsson, L., Hilgen, F.J., Langereis, C.G., Lourens, L.J., Verhallen, P.J.J.M. and Zijderveld, J.D.A. (1990). Late Gauss to early Matuyama invasions of *Neogloboquadrina atlantica* in the Mediterranean and associated record of climatic change. *Paleoceanography,* **5,** 239–252.